Structural Tuning of Ferromagnetism in a 3D Cuprate Perovskite

M. A. Subramanian,[1] A. P. Ramirez,[2] and W. J. Marshall[1]
[1]*DuPont Central Research and Development, Experimental Station, Wilmington, Delaware 19880-0328*
[2]*Bell Laboratories, Lucent Technologies, 600 Mountain Avenue, Murray Hill, New Jersey 07974-0636*
(Received 13 October 1998)

The perovskite $SeCuO_3$ is unusual for possessing (i) a very small *A*-site (Se^{4+}) radius, (ii) highly distorted Cu-O-Cu bond angles (α), and (iii) a ferromagnetic (FM) ground state. Negative chemical pressure is applied by replacing Se with Te in solid solution, causing a continuous transformation between the FM state and an antiferromagnetic (AFM) state. This is the first FM-AFM transformation to be controlled by a single microscopic parameter, the in-plane α, allowing a precise determination of the crossover angle ($\alpha_c = 127° \pm 0.5°$) between FM and AFM superexchange. [S0031-9007(99)08402-1]

PACS numbers: 75.30.Cr, 75.30.Et, 75.30.Kz, 75.50.Ee

The $3d$ transition metal oxides exhibit a wide variety of cooperative electronic states, among which high-T_c superconductivity in cuprates [1] and colossal magnetoresistance in manganites [2] are perhaps the best known examples. A growing interest in these compounds focuses attention on the microscopic interactions responsible for the low energy ground states. These interactions, such as correlation energy, exchange energy, and electron-phonon coupling energy form the basis from which microscopic Hamiltonians for cooperative motion are constructed.

With regard to the superexchange (SE) interaction in particular, the variability of atomic orbital overlap among the $3d$ ions in different structural configurations can lead to interactions of either sign and widely varying magnitude. The resulting systematics are summarized by a set of empirical rules which extend the Kramers-Anderson model of SE [3,4], i.e., electronic exchange between cations separated by intervening anions. Known as the Anderson-Goodenough-Kanemori (AGK) rules, their main utility is in providing approximate values for SE interaction signs and strengths [5,6]. For ions with orbital degeneracy, e.g., Cu^{2+}, the AGK rules must be modified to take into account orbital-ordering effects [7]. In La_2CuO_4, orbital ordering of the Jahn-Teller (JT) distorted Cu-O octahedra is uniaxial along the c-axis—the basal-plane Cu-O-Cu bond angle, α_{CuO}, is 180° and SE is antiferromagnetic (AFM) by wave function–orthogonality relations. However, in $La_4Ba_2Cu_2O_{10}$ [8], and $Sr_{0.73}CuO_2$ [9], antiferrodistortive ordering of the JT axis leads to $\alpha_{CuO} \approx 90°$, and a ferromagnetic (FM) interaction. It is not known precisely how the two ground states, FM and AFM, compete at intermediate angles. It generally assumed that a critical angle, $\alpha_c \approx 135°$, separates AFM and FM ground states [5] but there are no quantitative estimates, to our knowledge. From an empirical standpoint, the pyrochlores are the most frequently studied materials with bond angles in the range $\alpha \approx 135°$. However, these structures are geometrically frustrated and become spin-glass-like with effectively no disorder [10], making the identification of the dominant interaction type prohibitively difficult. Most other FM-AFM transitions, such as in the CMR-manganites, involve simultaneously changing several parameters, e.g., conduction electron density, lattice constant, and disorder, and involve interaction mechanisms other than SE. To our knowledge, continuous tuning between FM and AFM states by variation of a single parameter has not been previously demonstrated.

The focus of the present study is on the compound $SeCuO_3$, where the extremely small cation Se^{4+} leads to a highly distorted perovskite structure and consequently a FM ground state with $T_c = 25$ K [11]. We find that a small lattice perturbation, induced by substituting the larger Te^{4+} and Se^{4+}, is sufficient to drive the material into an AFM state ($T_N = 9$ K). This fortuitous structural condition creates a unique magnetic system and allows the precise determination of the value of α_{CuO} where the SE interaction changes sign.

Appropriate quantities of high purity SeO, TeO_2, and CuO were mixed together in an agate mortar and sealed in a gold capsule. The capsule was heated to 900 °C for 30 min at 5.8 GPa pressure in a tetrahedral anvil press and then rapidly cooled to room temperature before releasing the pressure. All of the peaks in powder x-ray diffraction (XRD) data for $Se_{1-x}Te_xCuO_3$ ($x = 0.0$ to 0.1) could be indexed with an orthorhombic unit cell (space group, *Pnma*) and no additional reflections due to impurities are observed. The refined lattice parameters and unit cell volume showed a systematic decrease with increasing Te substitution, consistent with the significantly smaller octahedral ionic radius for Se^{4+} when compared with Te^{4+} (Table I). Small single crystals of the $Se_{0.6}Te_{0.4}CuO_3$ phase were recovered and used for single-crystal x-ray diffraction (XRD) refinement at 296 K (Enraf-Nonius CAD-4 diffractometer, Ref. [12]). Our single crystal structure refinement [13] of $Se_{0.6}Te_{0.4}CuO_3$ showed expected systematic variation in cell parameters, bond distances, and bond angles, thus confirming the existence of continuous solid solution between $SeCuO_3$ and $TeCuO_3$

 0031-9007/99/82(7)/1558(4)$15.00

TABLE I. Lattice parameters of $Se_{1-x}Te_xCuO_3$ (refined in the space group, *Pnma*).

x	a (Å)	b (Å)	c (Å)
0.0	5.970(3)	7.331(4)	5.290(3)
0.2	5.971(3)	7.320(5)	5.361(3)
0.4	5.973(4)	7.311(4)	5.444(3)
0.5	5.976(3)	7.301(5)	5.475(4)
0.6	5.979(4)	7.286(5)	5.542(4)
0.8	5.980(3)	7.275(5)	5.601(4)
1.0	5.983(3)	7.269(4)	5.649(3)

phases. We have also determined the bond angles and bond distances for $Se_{1-x}Te_xCuO_3$ from powder diffraction data using the structural model obtained from single crystal structure refinements for $x = 0$, 0.4, and 1.0 (Tables I and II).

Both $SeCuO_3$ and $TeCuO_3$ adopt a distorted perovskite (ABO_3) structure, in which the A^{4+} cations occupy the larger A cation sites and Cu^{2+} at the B sites. The structure is composed of corner-shared CuO_6 octahedra to form a three dimensional network, and A cations reside in the cavities of this network. In an ideal perovskite structure, the A cation is in 12-fold coordination. In $SeCuO_3$ and $TeCuO_3$, the small size and strong covalent character of Se^{4+} and Te^{4+} pulls in 3 out of 12 oxygens, giving rise to AO_5 groups and an unusually large tilt of the CuO_6 octahedra (Fig. 1). In the case of ideal cubic perovskite structure the M-O-M angle is 180° as there is no tilt in BO_6 octahedral network (Fig. 1). The tilting of an octahedron is commonly observed in orthorhombic $GdFeO_3$-type perovskites resulting in M-O-M angles in the range 150°–180°. However, in $SeCuO_3$ and $TeCuO_3$, the angle is in the range 120°–130°, which is smaller than those in any of the ABO_3 perovskites. The above anomalously large deviation from an ideal perovskite is clearly due to Se^{4+} and Te^{4+} both having a nonbonded s-electron pair. In addition to the above tilting of octahedra, the CuO_6 octahedra also show large distortion with Cu-O distances varying from 1.9–2.6 Å and is due to the JT effect in Cu^{2+} (d^9) (Fig. 1).

TABLE II. Bond distances for $Se_{1-x}Te_xCuO_3$.

x	Cu-O(2) (Å) (±0.005)	Cu-O(2) (Å) (±0.004)	Cu-O1 (Å) (±0.004)
0.0[a]	2.521	1.919	2.090
0.2	2.534	1.922	2.088
0.4[a]	2.545	1.930	2.083
0.5	2.553	1.932	2.074
0.6	2.570	1.934	2.068
0.8	2.596	1.933	2.062
1.0[a]	2.610	1.937	2.060

[a]From single-crystal structure refinement.

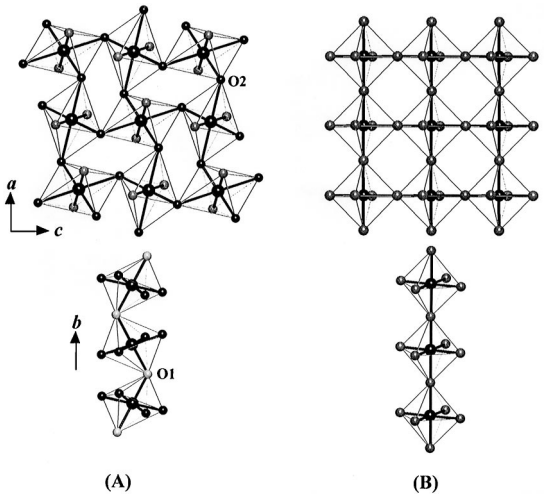

FIG. 1. (A) Projection of the crystal structure of orthorhombic $MCuO_3$ (M = Se, Te) showing the octahedral arrangement along ac plane and along b direction. The O1 and O2 atoms are marked. The arrangement results in a Cu-O-Cu angles in the range ~120°–130° (see text). (B) Projection of the ideal cubic perovskite structure showing 180° M-O-M interactions in all directions.

The d-c magnetization of the $Se_{1-x}Te_xCuO_3$ was measured in a commercial magnetometer in applied fields of 0.1 and 1 T. The specific heat was measured using a standard semiadiabatic heat-pulse technique.

In Fig. 2 is shown the magnetization, M, versus temperature for the compounds $Se_{1-x}Te_xCuO_3$. The $x = 0$ end member displays a saturation moment of

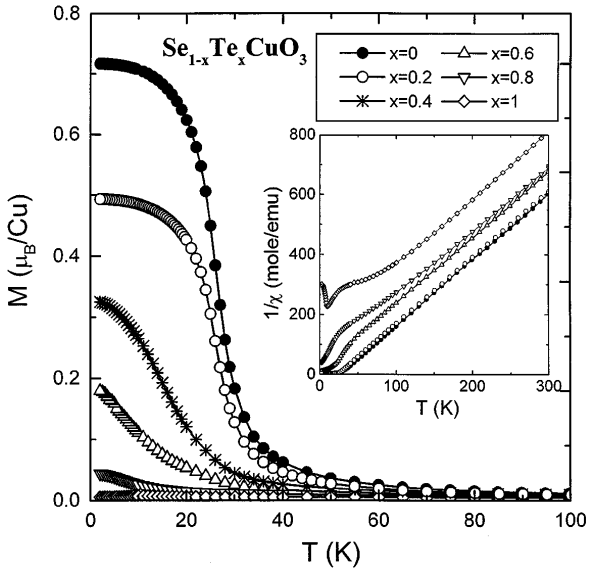

FIG. 2. Magnetization as a function of temperature at $H = 1$ T for $Se_{1-x}Te_xCuO_3$ for various x values. This shows the continuous decrease in M_{sat} as Te is substituted for Se. The inset shows the inverse susceptibility, $1/\chi$, for several of the samples, showing a continuous evolution in the Weiss temperature from FM-like for $x = 0$ to AFM-like for $x = 1$.

$M_{\rm sat}(2\ {\rm K}, 1\ {\rm T}) \approx 0.7\mu_B$ per Cu ion, similar to that reported earlier [10]. Since the dependence of $M_{\rm sat}$ on x appears from Fig. 2 to be continuous, it is reasonable to infer that the mechanism for moment reduction is already present to a small degree in the $x = 0$ sample, and we discuss this mechanism below. In the inset of Fig. 2 is shown $\chi^{-1}(T)$ for several samples. Concurrent with the decrease in $M_{\rm sat}$ is a sign change of the Weiss constant, θ_W, defined by the usual mean-field expression for the high-temperature susceptibility, $\chi^{-1} = C/(T - \theta_W)$, where C is the Curie constant. It is clear that, while the slope remains roughly constant ($\sim 1.8\mu_B$/Cu) for different x, θ_W, as determined from a fit to the high-temperature ($T > 100$ K) behavior goes continuously through zero. In the mean-field approximation, $\theta_W = (1/3)S(S + 1)zJ$, where S is the spin of the magnetic ion, z the number of nearest neighbors, and J the exchange constant for the magnetic interaction $H = J\sum S_i \cdot S_j$. Since S and z are independent of x, the variation of θ_W with x implies that the effective J value changes sign in the vicinity of $x = 0.5$. We emphasize, however, that this is an average value of J—below we address the effects of randomness of the magnetic interactions for nonintegral x.

In Fig. 3 is shown the specific heat divided by temperature, $C(T)/T$ for several samples. The magnetic field dependence of $C(T)/T$ is shown for the end members, $x = 0$ and 1. For $x = 0$ there is a sharp lambda-type anomaly whose peak locates the FM transition, $T_c = 25$ K. For nonzero H, the peak broadens and shifts up in temperature, typical for a ferromagnet. In contrast, the peak for $x = 1$ is not only at a lower temperature, but shifts down in a field, consistent with AFM ordering. In addition, this peak is significantly smaller in magnitude than for $x = 0$. A nonmagnetic isomorph is unavailable at present, so we estimate the lattice contribution to $C(T)/T$, by an AT^3 contribution where A is a constant determined by assuming that all the specific heat at 40 K, the upper bound of the present measurement, is due to lattice vibrations. Integrating the difference between this term and the measured $C(T)/T$ (see Fig. 3 inset), we find a value of 5.7 J/mole K, close to the total entropy for $s = 1/2$. Thus, although $M_{\rm sat}$ does not reach its full value, the C/T data are consistent with all the spins being involved in the FM phase transition at 25 K. Performing the same procedure for $x = 0$ and adjusting A to account for the mass difference between Se and Te, we find for the entropy up to 40 K only 3.1 J/mole K. Moreover, less than 1/3 of this entropy is lost in the critical region, below 15 K. The small entropy loss below T_N implies that a substantial amount of short range order exists at $T \geq T_N$ in $TeCuO_3$, a result also suggested by the broad high-temperature peak in C/T as shown in the inset of Fig. 3.

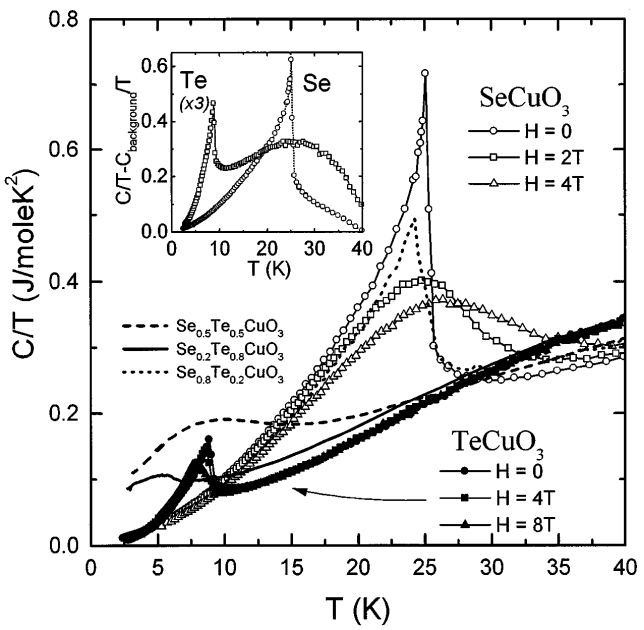

FIG. 3. Specific heat divided by temperature, C/T, for $SeCuO_3$ and $TeCuO_3$ at different values of applied field. Also shown are data on a few intermediate-x samples. The shift of entropy to high and low temperatures for $SeCuO_3$ and $TeCuO_3$ is behavior characteristic of FM and AFM transitions, respectively. The inset shows C/T with an approximate lattice contribution subtracted for the end members. The broad high-temperature feature for $TeCuO_3$ suggests substantial short-range order exists above the Neel transition.

In most of the intermediate-x samples a sharp anomaly in $C(T)$ was not observed—instead, a broad short-range-order peak between 5 and 15 K. The absence of sharp long-range-ordering anomalies, as seen for the $x = 0$ and 1 systems is consistent with a spin-glass-like state. A spin-glass state at each intermediate x is also implied by low-field magnetization studies which show hysteresis between zero-field-cooled and field-cooled values. Together, these results strongly suggest that the intermediate-x samples have spin-glass ground states, which in turn implies the existence of quenched site disorder. The most likely source of this disorder is a random strain field on the A-cation sites, influencing the magnetism through the variation of local values of $\alpha_{\rm CuO}$. It is likely that the FM-AFM transition is second order because the $x = 0$ sample shows an intermediate $M_{\rm sat}$ despite there being no quenched disorder.

In order to extract a critical angle for change of interaction sign, FM-AFM, we first recognize there are two distinct bonding types in $Se(Te)CuO_3$ due to antiferrodistortive ordering of the JT elongation axis (Fig. 1): These are labeled Cu-O1-Cu along the b axis and Cu-O2-Cu in the ac plane. Because the JT axis is closer to lying in the ac plane than along the b axis, the bonding pattern resembles that of $La_4Ba_2Cu_2O_{10}$, although the angles are far away from 90°. Since $SeCuO_3$ is nearly fully FM, both angle types are on the FM side of their respective critical values. Also, both because $\alpha_{\rm CuO1} \approx 122°$, which is significantly less than $\alpha_{\rm CuO2}$ for either Se or Te

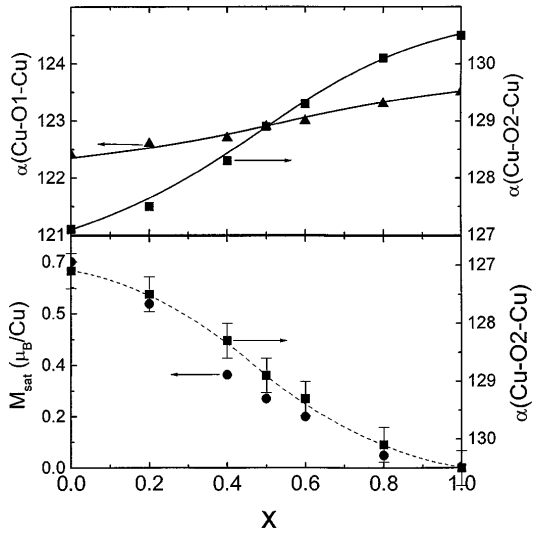

FIG. 4. Top panel: Cu-O-Cu bond angle variation for the ac plane angles (Cu-O2-Cu) and the b axis angles (Cu-O1-Cu); Bottom panel: Comparison of variation of $M_{\rm sat}$ and ac-plane angle with Te concentration.

compounds, and because $\alpha_{\rm CuO1}$ changes little upon substituting Te for Se, it is reasonable to assume that the Cu-O1-Cu bond remains FM even for $TeCuO_3$. In this case, the interaction sign change is caused by the change in $\alpha_{\rm CuO2}$ from 127.1° for $x = 0$ to 130.5° for $x = 1$. In Fig. 4 is shown the evolution of $M_{\rm sat}$, $\alpha_{\rm CuO1}$, and $\alpha_{\rm CuO2}$ as x is varied. To define α_c, we assume that the bond-overlap condition which determines J is linear as a function of angle over the small region where $M_{\rm sat}$ changes. Linearity of $J(\alpha)$ over a small α span is supported by the overall change of (25 K)(180° − 127°)/3° = 440 K which is on the order of transition temperatures found in cuprates with 180° bonds. Thus, we identify $x(M_{\rm sat} = 0.5\mu_B)$ as the concentration where the wave function–orthogonality rules are marginalized to find $\alpha_c = 127.5° \pm 0.5°$ for the transition between FM and AFM bonding. Note that this angle is significantly less than that usually assumed as the crossover angle, 135°.

Finally, we can understand the shortfall in the magnitude of $M_{\rm sat}$ for $x = 0$ from the full Cu^{2+} moment of 1 μ_B as a result of the competition between AFM and FM tendencies. When the respective nearest-neighbor exchange processes cancel each other, as they might at intermediate Cu-O-Cu bond angles, longer-range interactions become important. In such a situation spin canting can occur, providing a mechanism for a continuous crossover in ground state properties between AFM and FM end points. If so, this spin canting can exist not only for intermediate x, but for $x = 0$ and should be observable with neutron diffraction.

In conclusion, we have shown that the Cu-O-Cu bond angle in $SeCuO_3$ is close to the critical angle where the interaction is expected to change sign and we have succeeded in accessing a sign change in the average exchange interaction by Te substitution. To our knowledge, this is the first realization of the ability to vary this M-O-M angle continuously through the critical value leaving the M cation and anion unchanged, in any perovskite structure.

We wish to acknowledge fruitful discussions with P. Littlewood and C. Varma.

[1] R. Beyers and T. M. Shaw, *Solid State Physics*, edited by H. Ehrenreich and D. Turnbull (Academic Press, New York, 1989), Vol. 42, pp. 91–212.
[2] A. P. Ramirez, J. Phys. Condens. Matter **9**, 8171 (1997).
[3] H. A. Kramers, Physica (Utrecht) **1**, 182 (1934).
[4] P. W. Anderson, Phys. Rev. **79**, 705 (1950).
[5] J. B. Goodenough, Phys. Rev. **100**, 564 (1995); *Magnetism and the Chemical Bond* (Wiley, New York, 1963).
[6] J. Kanemori, J. Phys. Chem. Solids **10**, 87 (1959).
[7] D. I. Khomskii and K. I. Kugel, Solid State Commun. **13**, 763 (1973).
[8] F. Mizuno, H. Masuda, I. Hirabayashi, S. Tanaka, M. Hasegawa, and U. Mizutani, Nature (London) **345**, 788 (1990).
[9] A. Shengelaya, G. I. Meijer, J. Karpinski, G. Zhao, H. Schwer, E. M. Kopnin, C. Rossel, and H. Keller, Phys. Rev. Lett. **80**, 3626 (1998).
[10] J. E. Greedan, M. Sato, X. Yan, and F. S. Razavi, Solid State Commun. **59**, 895 (1986).
[11] K. Kohn, K. Inoue, O. Horie, and S. Akimot, J. Solid State Chem. **18**, 27 (1976).
[12] M. A. Subramanian, B. H. Toby, A. P. Ramirez, W. J. Marshall, A. w. Sleight, and G. H. Kwei, Science **273**, 81 (1996).
[13] Data for the single-crystal, x-ray structure determination were collected with an Enraf-Nonius CAD4 x-ray diffractometer equipped with a monochromatic Mo $K\alpha$ source. Orthorhombic cell parameters for both samples were indexed from twenty-five diffraction maxima. Intensity data sets were then collected using pure ω-scans over a full sphere of reflections. The structures were refined in space group *Pnma* (No. 62) by full-matrix least-squares refinement. Biweights were used in the final refinement where $R_w = [\sum(|F_0| - |F_c|)^2/\sum w|F_0|^2]^{1/2}$ with w proportional to $[s^2(I) + 0.0009I^2]^{-1/2}$. The final R factors are 0.029 and 0.025 for $Se_{0.6}Te_{0.4}CuO_3$ and $TeCuO_3$, respectively. The final positional parameters for $Se_{0.6}Te_{0.4}CuO_3$ are (Se, Te), $x = 0.0216(5)$, $y = 0.25$, $z = 0.0324(5)$; Cu, $x = 0.0$, $y = 0.0$, $z = 0.50$; O(1); O(1), $x = 0.0607(6)$; $y = 0.25$; $z = 0.333(1)$; O(2), $x = 0.1986(10)$; $y = 0.0657(9)$; $z = -0.095(1)$. We have re-refined the structure of $TeCuO_3$ to obtain more accurate bond distances and bond angles given in Ref. [12]. Further details on the structure determination of these phases will be published elsewhere.